Transition Metal Chemistry (2023) 48:377–387
https://doi.org/10.1007/s11243-023-00550-x

Synthesis, spectroscopic characterization, and photophysical properties of new *p*-anisolylthiol-functionalized platinum(II) bis(alkenylarylalkynyl) complexes

Md. Mostafizur Rahman[1] · Tanjila Islam[2] · Md. Amran-Al-Taz Khan[2] · Muhammad Younus[1,2] · Dababrata Paul[3] · Md. Sajib Joardar[1] · Akiya Ogawa[4,5]

Received: 9 April 2023 / Accepted: 5 August 2023 / Published online: 16 August 2023

Abstract

A series of organic sulfur-functionalized *trans*-platinum(II) bis(alkenylarylalkynyl) complexes, having one anisolylthio group with general formula *trans*-[$(PEt_3)_2Pt\{C{\equiv}C–Ar–CH{=}CH(SC_6H_4–OCH_3)\}_2$], **(2a-2d)**, (Ar = phenylene/biphenylene/2,5-dimethylphenylene/2,5-dimethoxyphenylene) was synthesized in excellent yields. All the new platinum(II) complexes have been fully characterized by physico-chemical and spectroscopic methods. Photophysical properties of the complexes were studied by absorption and emission spectroscopy. The lowest energy absorption band for the complexes, in the UV/Vis spectra, in THF solution, at room temperature, **2a-2d** was observed in the range 355–391 nm, which depend on the spacers in the acetylide ligand e.g., the absorption of 2d is red shifted to 391 nm for the donor (OCH_3) substituents in phenyl spacer. These absorptions originated predominantly from π–π*orbitals of acetylide ligand with significant contribution from the platinum dπ orbital as evident from the HOMO and LUMO, obtained from TD-DFT calculations. Fluorescence was observed in all complexes at room temperature in the range 400–428 nm with PLQY of 2–5%. At 77 k, the complexes **2a-2b** only exhibited phosphorescence in the range 579–585 nm, but there is no phosphorescence at ambient temperature.

Introduction

There has been a lot of interest in the synthesis of small, medium, and large π-conjugated acetylenic materials due to the growing interest in the production of novel classes of materials with exciting optical properties and applications [1–3]. The potential uses of transition metal acetylide complexes and polymers in various areas of materials science, such as organic light emitting diodes [4, 5], photovoltaic cells [6–8], and field-effect transistors [9], have sparked significant interest concurrently. Over the last three decades, there has been a growing interest in the design of conjugated materials that exhibited a range of material properties such as linear and non-linear optics [10, 11], organo-gelators [12, 13], liquid crystals [14, 15], photovoltaic behavior [16–18], depending on the structure of the molecules, and the nature of the intermolecular interactions as well as their long-lived triplet excited states [19, 20]. The unique physical properties of transition metal acetylides are caused by their rigid rod structures and prominent π-electron conjugation involving the metal's *d*-electrons and the π-system of the carbon–carbon triple bond [1–3]. On the other hand, the chemical and physical properties of carbon-rich organic oligomers often

Mostafizur Rahman, Tanjila Islam, Amran-Al-Taz Khan have equally contributed to this work.

✉ Md. Mostafizur Rahman
mostafiz-che@sust.edu

[1] Department of Chemistry, School of Physical Sciences, Shahjalal University of Science & Technology, Sylhet 3114, Bangladesh

[2] Department of Chemistry, University of Texas at San Antonio, San Antonio, TX 78249, USA

[3] Department of Chemistry, Bangabandhu Sheikh Mujibur Rahman Science & Technology University, Gopalgonj 8100, Bangladesh

[4] Department of Applied Chemistry, Graduate School of Engineering, Osaka Metropolitan University, 1-1 Gakuen-cho, Nakaku, Sakai, Osaka 599-8531, Japan

[5] Department of Applied Chemistry, Graduate School of Engineering, Osaka Prefecture University, 1-1 Gakuen-cho, Nakaku, Sakai, Osaka 599-8531, Japan

cannot be exploited due to their poor solubility, but this can be improved by incorporating alkyl substituent's on the ligand as well as metal center on the oligomeric backbone [21]. The presence of platinum as a heavy metal induces strong spin–orbit coupling which in turn accelerates the inter system crossing by reducing the singlet–triplet energy gap [4, 5, 16]. Multi-functionalized platinum(II) bis(acetylide) complexes are well known in the field of photophysics due to their extensive photophysical characteristics [22–24].

In order to synthesize a wide variety of transition metal alkynyl complexes, several M–C≡C bond-forming reactions are available [25, 26]. Due to the π-unsaturated nature of alkynyl groups and their linear shape when connected to metal centers, metal alkynyls are easily coupled to create linear complexes, oligomers, and polymers with potential uses in materials science [1–3]. Particularly, extensive research has been done on the square planar geometry of the functionalized alkynyl system of platinum(II) complexes [16, 27–30].

Recently, we have reported the palladium catalyzed synthesis of novel organosulfur-functionalized *trans*-platinum(II) bis(acetylide) complexes having two phenylthio groups in each alkenyl backbone [31] and the photochemical synthesis of novel organoselenium-functionalized *trans*-platinum(II) bis(acetylide) complexes having two phenylseleno groups in each alkenyl backbone [32]. The radical facilitated thiolation of terminal alkyl/arylacetylenes is well-precedented in synthetic organic chemistry [33, 34], which is rare in organometallic chemistry. Our group only reported this type of reactions recently for the functionalization of platinum acetylides [35–37]. Among the π-conjugated organometallic materials, the conjugated polymers are promising for their ease of preparation, solution process ability and wide range of materials properties [1–3], but it has not been well regarded to small molecules [12, 16, 38, 39]. Therefore, researchers focused on the photochemical synthesis, spectroscopic characterization and optoelectronic properties of four new *p*-anisolylthiol-functionalized *trans*-platinum(II) bis(alkenylarylalkynyl) complexes, *trans*-$[(Et_3P)_2Pt\{C{\equiv}C–Ar–CH{=}CH(SC_6H_4OCH_3\text{-}p)\}_2]$, **(2)** (where, Ar = phenylene/biphenylen/2,5-dimethylphenylene/2,5-dimethoxyphenylene), bearing one anisolylthio group in each alkenyl backbone, which are stabilized by the presence of monodentate ancillary phosphine ligands.

Experimental

Material and methods

All reactions were performed under a nitrogen atmosphere. Solvents were dried, distilled by using appropriate drying agents and degassed before use [40]. All chemicals, except where stated, were purchased from commercial sources and used without further purification. The compounds $HC{\equiv}C–C_6H_4–C{\equiv}CH$ [41], $HC{\equiv}C–C_6H_4–C_6H_4–C{\equiv}CH$ [41], $HC{\equiv}C–C_6H_2(p\text{-}CH_3)_2–C{\equiv}CH$ [41], $HC{\equiv}C–C_6H_2(p\text{-}OCH_3)_2–C{\equiv}CH$ [41], *trans*-$[(Et_3P)_2Pt\{C{\equiv}C–C_6H_4–C{\equiv}CH\}_2]$ [25], *trans*-$[(Et_3P)_2Pt\{C{\equiv}C–C_6H_4–C_6H_4–C{\equiv}CH\}_2]$ [25], *trans*-$[(Et_3P)_2Pt\{C{\equiv}C–C_6H_2(p\text{-}CH_3)_2–C{\equiv}CH\}_2]$ [25], and *trans*-$[(Et_3P)_2Pt\{C{\equiv}C–C_6H_2(p\text{-}OCH_3)_2–C{\equiv}CH\}_2]$ [25] were prepared according to literature methods. NMR spectra were recorded on Bruker 400 MHz FT NMR spectrometer in $CDCl_3$. $^{31}P\{^1H\}$ NMR spectra were referenced to external trimethylphosphite. ^1H NMR spectra were referenced to internal TMS, and $^{13}C\{^1H\}$ NMR spectra were referenced to solvent resonances. Infrared spectra were recorded on Shimadzu FTIR prestige 21 spectrometer by using KBr pellets, and ESI-HR mass spectra were recorded on JEOL JMS-T100LC spectrometer. Microanalyses were performed on the analytical section of BCSIR, Dhaka. The UV visible absorption spectrum was recorded using a Shimadzu UV-1800 dual-beam spectrophotometer, and steady-state emission photoluminescence measurements were done using an Edinburgh FLS1000 spectrophotometer. Low temperatures emission was obtained using fingertip Dewar contained liquid nitrogen. The absolute quantum yield of the complexes was measured using an integrating sphere. Fluorescence lifetime decay was measured from a Pico Quant FT300 time correlated single photon correlation (TCSPC) instrument using Ti: Sapphire laser source. DFT and TD-DFT calculations were performed using Gaussian 16, with B3LYP functionality and SDD basis set. The calculations were conducted using the University of Texas HPC system. Column chromatography was performed on silica gel.

Synthesis of complex 2a

A mixture of *trans*-$[(Et_3P)_2Pt\{C{\equiv}C–C_6H_4–C{\equiv}CH\}_2]$ (**1a**) (0.068 g, 0.1 mmol) and *p*-anisolylthiol (0.035 g, 0.25 mmol) was added in chloroform (0.6 mL) and degassed under nitrogen atmosphere in a sealed tube. The resulting mixture was irradiated under tungsten lamp 500 W for 3 h (cool water was passed over the sealed tube to maintain room temperature). The completion of the reaction was examined by TLC and IR. The solvent was removed under reduced pressure. The resulting crude product was purified by silica column chromatography, eluting with hexane and dichloromethane, and the title complex **2a** was isolated as a yellow solid in 98% yield (0.094 g), *E*/*Z* ratio: 60/40. IR (solid state, KBr): ν2099 (C≡C) cm^{-1}; ^1H NMR (400 MHz, $CDCl_3$): (*E*/*Z* ratio: 60/40): δ 7.41–6.87 (m, 16H, Ar–H, SAr-H), 6.73 (d, 1.20 × 1H, $J_{H–H}$ = 15.2 Hz), 6.48 (d, 1.20 × 1H, $J_{H–H}$ = 15.2 Hz), 6.42 (d, 0.80 × 1H, $J_{H–H}$ = 10.8 Hz), 6.31 (d, 0.80 × 1H, $J_{H–H}$ = 11.2 Hz), 3.79 (s), 3.78 (s) {6H,

SAr-OCH_3-*p*}, 2.20–2.14 (m, 12H, CH_2) and 1.26–1.16 (m, 18H, CH_3); $^{13}C\{^1H\}$ NMR (100 MHz, $CDCl_3$): δ 8.2, 16.2, 55.3, 109.2, 109.3, 109.6, 109.8, 114.7, 114.7, 124.1, 124.8, 125.4, 125.7, 126.9, 127.0, 127.4, 127.7, 128.2,129.4, 130.6, 131.0, 132.7, 133.0, 133.3, and 159.3; $^{31}P\{^1H\}$ NMR (161.83 MHz, $CDCl_3$): δ11.6 (J_{Pt-P} = 2370 Hz); ESI-HRMS $[M]^+$ *m*/*z* = 962.2823 (100%), Calc. mass: 962.0932, Anal. Calc. for $C_{46}H_{56}O_2P_2PtS_2$: C, 57.43; H, 5.87%. Found: C, 57.39; H, 5.98%.

Synthesis of complex 2b

The same procedure was followed for the synthesis of platinum(II) complex **2b** as previously applied for the synthesis of **2a**, but platinum(II) bis(acetylide) complex **1b**, *trans*-$[(Et_3P)_2Pt\{C{\equiv}C–C_6H_4–C_6H_4–C{\equiv}CH\}_2]$ was used instead of *trans*-$[(Et_3P)_2Pt\{C{\equiv}C–C_6H_4–C{\equiv}CH\}_2]$ (**1a**), and the reaction was carried out for 5 h. The resulting crude product was purified by silica column chromatography, eluting with hexane and dichloromethane, and the title complex **2b** was isolated as a yellow solid in 90% yield (0.100 g), *E*/*Z* ratio: 63/37. IR (solid state, KBr): ν 2097 (C≡C) cm^{-1};^1H NMR (400 MHz, $CDCl_3$): (*E*/*Z* ratio: 63/37): δ 7.62–7.32 (m, 20H, Ar–H, SAr-H), 6.92–6.83{5.26H (m, 4H, SAr-H; d, 1.26 × 1H), 6.53 (d, 1.26 × 1H, J_{H-H} = 13.6 Hz), 6.50 (d, 0.74 × 1H, J_{H-H} = 8.8 Hz), 6.40 (d, 0.74 × 1H, J_{H-H} = 10.4 Hz), 3.81 (s), 3.80 (s) {6H, SAr-OCH_3-*p*}, 2.21–2.16 (m, 12H, CH_2) and 1.29–1.19 (m, 18H, CH_3); $^{13}C\{^1H\}$ NMR (100 MHz, $CDCl_3$): δ 8.3, 16.3, 55.3, 109.1, 109.4, 114.77, 114.8, 124.5, 125.3, 125.5, 126.1, 126.2, 126.4, 126.5, 126.7, 126.8, 127.9, 128.2, 128.5, 129.0, 131.2, 132.9, 133.3, 135.3, 135.3, 136.9, 137.0, 139.3, 139.7, 159.4, and 159.5;$^{31}P\{^1H\}$ NMR (161.83 MHz, $CDCl_3$): δ11.6 (J_{Pt-P} = 2396 Hz); ESI-HRMS $[M]^+$*m*/*z* = 1114.3478 (100%), Calc. mass: 1114.2851, Anal. Calc. for $C_{58}H_{64}O_2P_2PtS_2$: C, 62.52; H, 5.79%. Found: C, 62.24; H, 5.87%.

Synthesis of complex 2c

The synthetic procedure was the same as for the synthesis of platinum(II) complex **2a**, but platinum(II) bis(acetylide) complex **1c**, *trans*-$[(Et_3P)_2Pt\{C{\equiv}C–C_6H_2(CH_3–p)_2–C{\equiv}CH\}_2]$, was used instead of *trans*-$[(Et_3P)_2Pt\{C{\equiv}C–C_6H_4–C{\equiv}CH\}_2]$, **1a**, and the reaction was carried out for 3 h. The resulting crude product was purified by silica column chromatography, eluting with hexane and dichloromethane, and the title complex **2c** was isolated as a pale yellow solid in 99% yield (0.101 g), *E*/*Z* ratio: 50/50. IR (solid state, KBr): ν 2091 (C≡C) cm^{-1}; ^1H NMR (400 MHz, $CDCl_3$): (*E*/*Z* ratio: 50/50): δ 7.40–7.36 (m, 5H, SAr-H, Ar–H), 7.18 (s, 1H, Ar–H), 7.12 (s, 1H, Ar–H), 7.05 (s, 1H, Ar–H), 6.88 (d, 2H, SAr-H, J_{H-H} = 6.4 Hz), 6.85 (d, 2H, SAr-H, J_{H-H} = 6.4 Hz), 6.76 (d, 1 × 1H, J_{H-H} = 15.6 Hz), 6.66 (d, 1 × 1H, J_{H-H} = 15.2 Hz), 6.54 (d, 1 × 1H, J_{H-H} = 10.4 Hz), 6.35 (d, 1 × 1H, J_{H-H} = 10.8 Hz), 3.79 (s), 3.78 (s) {6H, SAr-OCH_3-*p*}, 2.44 (s, 3H, Ar-CH_3-*p*), 2.36 (s, 3H, Ar-CH_3-*p*), 2.24 (s), 2.22 (s){6H, Ar-CH_3-*p*)}, 2.18–2.11 (m, 12H, CH_2) and 1.24–1.14 (m, 18H, CH_3); $^{13}C\{^1H\}$ NMR (100 MHz, $CDCl_3$): δ 8.2, 16.2, 19.1, 19.3, 20.7, 20.9, 55.2, 108.5, 108.7, 114.6, 114.7, 124.4, 124.5, 125.4, 125.5, 127.1, 127.1, 127.6, 127.6, 127.7, 127.8, 127.9, 128.0, 128.8, 131.6, 131.7, 131.7, 132.0, 132.0, 132.5, 132.6, 132.7, 132.9, 135.6, 136.1, and 159.1; $^{31}P\{^1H\}$ NMR (161.83 MHz, $CDCl_3$): δ 12.2 (J_{Pt-P} = 2384 Hz); ESI-HRMS $[M]^+$ *m*/*z* = 1018.3453 (100%), Calc. mass: 1018.1995, Anal. Calc. for $C_{50}H_{64}O_2P_2PtS_2$: C, 58.98.89; H, 6.34%. Found: C, 58.84; H, 6.44%.

Synthesis of complex 2d

The same procedure as for the platinum(II) complex **2a** was followed for the synthesis of **2d**, but platinum(II) bis(acetylide) complex **1d**, *trans*-$[(Et_3P)_2Pt\{C{\equiv}C–C_6H_2(OCH_3-p)_2–C{\equiv}CH\}_2]$, was used instead of *trans*-$[(Et_3P)_2Pt\{C{\equiv}C\text{-}C_6H_4\text{-}C{\equiv}CH\}_2]$, **1a**, and the reaction was carried out for 3 h. The resulting crude product was purified by silica column chromatography, eluting with hexane and dichloromethane, and the title complex **2d** was isolated as a deep yellow solid in 88% yield (0.096 g), *E*/*Z* ratio: 65/35. IR (solid state, KBr): ν 2094 (C≡C) cm^{-1}; ^1H NMR (400 MHz, $CDCl_3$): (*E*/*Z* ratio: 65/35): δ 7.42–7.38 (m, 4H, SAr-H),7.18 (s, 0.70 × 1H, Ar–H), 6.90–6.73 [m, 10.6 × 1H, {SAr-H (4H), Ar–H (3.3 × 1H), –CH = CH– (3.3 × 1H)}], 6.34 (d, 0.70 × 1H, J_{H-H} = 10.4 Hz), 3.85–3.75 (18H, SAr-OCH_3-*p*, Ar-OCH_3-*p*), 2.27–2.22 (m, 12H, CH_2) and 1.27–1.17 (m, 18H, CH_3); $^{13}C\{^1H\}$ NMR (100 MHz, $CDCl_3$): δ8.4, 16.1, 55.3, 56.1, 56.2, 56.3, 105.4, 109.0, 111.8, 114.7, 115.2, 116.0, 117.9, 120.5, 123.1, 123.2, 123.2, 124.7, 124.8, 125.3, 125.4, 125.5, 126.9, 127.0, 132.7, 132.8, 150.3, 150.4, 154.0, 154.4, 159.2, and 159.3; $^{31}P\{^1H\}$ NMR (161.83 MHz, $CDCl_3$): δ11.8 (J_{Pt-P} = 2395 Hz); ESI-HRMS $[M]^+$ *m*/*z* = 1082.3258 (100%), Calc. mass: 1082.1971, Anal. Calc. for $C_{50}H_{64}O_6P_2PtS_2$: C, 55.49; H, 5.96%. Found: C, 55.37; H, 6.03%.

Results and discussion

Syntheses

Under UV light irradiation, the platinum(II) complex, which has an extended ethynyl ligand *trans*-$(Et_3P)_2Pt\{C{\equiv}C–C_6H_4–C{\equiv}CH\}_2$ (**1a**), was reacted with *p*-anisolylthiol [34, 35], and provided a yellow solid platinum(II) bis(alkenylarylalkynyl) complex (**2a**) in excellent yield

(98%, isolated yield; Table 1, entry 1; Scheme 1). *p*-Anisolylthiol photolysis requires UV light with a wavelength between 300 and 250 nm, which was achieved using a 500 W tungsten lamp [42]. According to Oliver et al. (2012), the photodissociation of *para*-substituted thiophenols took place at ~ 280 nm. They discovered that UV irradiation in the range 305 > phot > 240 nm causes the fission of the S–H bond and the production of the *p*-YPhS˙ radical (Y = CH_3/F/OCH_3) [42]. The structure of the complex was identified by IR, multi-nuclear NMR spectroscopy, and ESI-HR mass spectrometry as well as elemental analysis.

With the analogous reaction conditions (Table 1, entry 1), various platinum(II) bis(acetylides), *trans*-$(Et_3P)_2Pt(C{\equiv}C–Ar–C{\equiv}CH)_2$, (**1**) (Ar = biphenylene/2,5-dimethylphenylene/2,5-dimethoxyphenylene) were also examined (Scheme 1) by adding *p*-anisolylthiol under UV radiation. The outcome of these reactions is general, which gave expected *p*-anisolylthiol-functionalized complexes, **2b-2d** (Table 1). This methodology tolerates *trans*-platinum(II) bis(acetylide) complexes, with extended ethynyl ligand of diterminal alkynes, containing aryl rings as well as substituted aryl rings.

All the reactants were converted to thiolated products within 3 to 5 h under irradiation with UV light (Table 1). The crude products were purified by silica column chromatography, eluting with hexane/dichloromethane. The highly pure *E/Z* isomers are inseparable mixtures which displayed a single spot on TLC plate. The pure compounds were isolated as yellow to deep yellow solids in 88–99% yields. The complexes are soluble in common organic solvents but are insoluble in hexane. The *p*-anisolylthiol-functionalized *trans*-platinum(II) bis(alkenylarylalkynyl) complexes are air-stable. In our previous study, the reaction of benzenethiol/*p*-tolylthiol with platinum(II) bis(acetylide) provided the thiolated complexes in 70–90% yields [35–37]. In the present study, methoxy substituted thiol gives much higher yields (88–99%). The *trans*-platinum(II) complexes (**2**) provided satisfactory elemental analyses. The products were also characterized by IR, ^1H, ^{13}C and ^{31}P NMR spectroscopy and positive ESI-HR $[M]^+$ mass spectrometry.

Stereochemistry

The newly synthesized complexes exhibited good regioselectivity. The isomeric nature (*E/Z*) of the complexes was ascertained using the measured values of the coupling constant of the vinylic protons, which are made obvious by ^1H NMR spectroscopic analysis (Table 1). For instance, the

Table 1 Synthesis of *p*-anisolylthiol-functionalized various *trans*-platinum(II) bis(acetylides)

Entry	Platinum(II) acetylide, *trans*-$(Et_3P)_2Pt\{C{\equiv}C–Ar–C{\equiv}CH\}_2$, **1**	Thiol (XSH)	Duration (h)	Product, **2**[i] (%), (*E/Z*)[a]
1	Ar = phenylene, **1a**	*p*-$MeOC_6H_4SH$	3	98 (**2a**) (60/40)
2	Ar = biphenylene,**1b**	*p*-$MeOC_6H_4SH$	5	90 (**2b**) (63/37)
3	Ar = 2,5-dimethylphenylene, **1c**	*p*-$MeOC_6H_4SH$	3	99 (**2c**) (50/50)
4	Ar = 2,5-dimethoxyphenylene, **1d**	*p*-$MeOC_6H_4SH$	3	88 (**2d**) (65/35)

Reactions were carried out in chloroform solvent upon irradiation by using **1**, *trans*-$(Et_3P)_2Pt\{C{\equiv}C–Ar–C{\equiv}CH\}_2$ (0.1 mmol) and *p*-anisolylthiol (0.25 mmol)

[i]Isolated yields

[a]Inseparable mixture of *E/Z* isomers were estimated by ^1H NMR spectroscopy

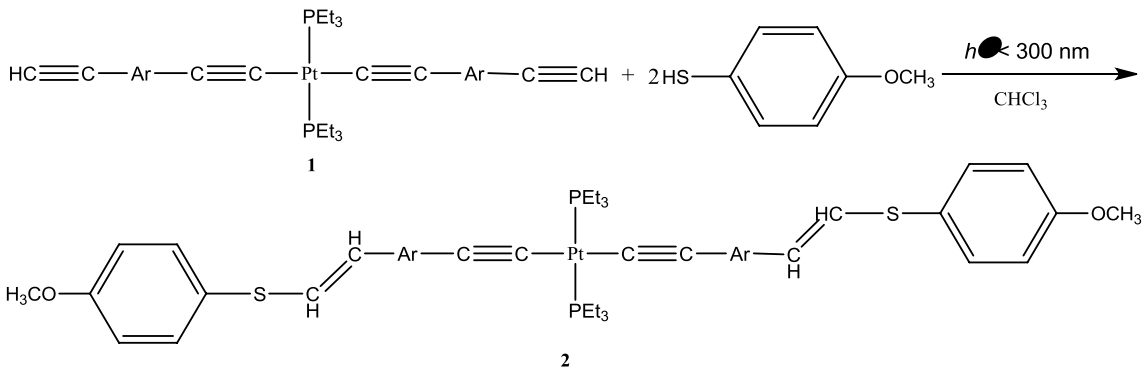

Ar = phenylene (**a**), biphenylene (**b**), 2,5-dimethylphenylene (**c**), and 2,5-dimethoxyphenylene (**d**)

Scheme. 1 Synthetic route of *p*-anisolylthiol-functionalized various *trans*-platinum(II) bis(alkenylarylalkynyl) complexes

observed values of the vinylic protons coupling constant for the *trans*-platinum(II) complex **2a** are 10.8 and 11.2 Hz for *Z* isomers and 15.2 and 15.2 Hz for *E* isomers (Table 2) [36]. The *E* isomer is preferred over the creation of the Z isomer.

Characterization

The new organometallic complexes were characterized by using traditional methodologies such as elemental analysis, IR, ^{1}H, $^{13}C\{^{1}H\}$ and $^{31}P\{^{1}H\}$ NMR spectroscopy and mass spectrometry (positive $[M]^{+}$ ion in ESI-HR MS). The selected basic spectroscopic data for all the new compounds in this study are summarized in Table 2.

The platinum-alkyne carbon bond (Pt–C≡C) is confirmed to be sustained by a sharp single absorption band on the range of 2099–2091 cm^{-1} in the IR spectra of the *p*-anisolylthiol-functionalized *trans*-platinum(II) bis(alkenylarylalkynyl) complexes **2**. In the IR spectra, the absence of the terminal ≡C–H absorption band confirms the completion of the reaction. As for example, platinum(II) complex **2a** displayed a sharp single absorption band at 2099 cm^{-1}, which is assigned to ν(C≡C) stretching vibration (Table 2) and showed no bands in the range 3200–3300 cm^{-1}, which is the characteristic region for the ≡C–H stretching vibration [32]. It is clear that the anisolylthiol and terminal acetylenic group had a specific reaction.

The vinyl protons exhibit new peaks in the range of 6.31–6.92 ppm in the ^{1}H NMR spectra of platinum(II) bis(alkenylarylalkynyl) complexes **2** (Fig. 1). For instance, platinum(II) complex **2a** displayed two sets of doublets at 6.73 and 6.48 ppm for *E* isomer, and 6.42 and 6.31 ppm for *Z* isomer (Table 2) [36, 37, 43]. On the other hand, in the ^{1}H NMR spectra of complexes **2**, there was no signal at about 3 ppm, which is the characteristic region for the terminal alkyne proton ≡C–H. In the ^{1}H NMR spectra of platinum(II) complex **2a**, the methyl protons of two isomers (*E*/*Z*) of the *p*-anisolylthio group were seen as two singlets at 3.79 and 3.78 ppm. In each case, signals from the *p*-anisolylthio moiety, organic spacers, and ethyl phosphine protons likewise displayed peaks in the anticipated area. In ^{1}H NMR spectra, platinum(II) complex **2b** showed three vinyl proton doublets and one vinyl proton overlapped with the aromatic ring of the organic spacer, platinum(II) complex **2c** showed four vinyl proton doublets, platinum(II) complex **2d** showed one vinyl proton doublet and three vinyl protons overlapped with the aromatic ring of the organic spacers, and all other protons display peaks at the expected region.

The $^{31}P\{^{1}H\}$ NMR spectra of each platinum(II) bis(alkenylarylalkynyl) complexes **2** showed the expected signals consisting of three lines due to coupling with ^{195}Pt, such as, platinum(II) complex **2c** displayed a sharp singlet at 12.2 ppm along with two satellites positions on 19.5 and 4.8 ppm (Fig. 2). The *trans* geometry around the platinum-diphosphine centers was confirmed by $^{31}P\{^{1}H\}$ NMR spectroscopy based on the J_{Pt-P} coupling constant [36, 37]. The *E*/*Z* intimate mixtures mutually displayed a sharp singlet in $^{31}P\{^{1}H\}$ NMR (Table 2), because in both cases (*E*/*Z*), geometry is only associated with the terminal alkene, which is isolated from the phosphine ligands. The J_{Pt-P} values obtained, *i.e.*, 2370, 2396, 2384, and 2395 Hz for the platinum(II) complexes **2a**, **2b**, **2c**, and **2d**, respectively, are in agreement by the values earlier reported for other square planar platinum(II) complexes which bearing *trans* geometry [44, 45]. $^{13}C\{^{1}H\}$ NMR spectrum was also performed for each complex and display signals in the expected region.

The molecular formula of the newly synthesized complexes was also recognized by the intense molecular ion $[M]^{+}$ peaks in the positive ion ESI-HR mass spectra

Table 2 Some spectroscopic data for the *trans*-platinum(II) bis(alkenylarylalkynyl) complexes **2a-d**

Platinum(II) complexes (**2**)	IR (KBr) υ(C≡C) (cm^{-1})	^{1}H NMR (ppm)[a] [–CH=CH(SX)], vinyl proton (Doublet = d)[c] (*E*/*Z*)	$^{31}P\{^{1}H\}$ NMR (ppm)[b]	ESI-HR (Calc.) *m*/*z*	Mass
trans-[$(Et_3P)_2Pt\{C{\equiv}C{-}C_6H_4{-}CH{=}CH(SC_6H_4OMe\text{-}p)\}_2$] (**2a**)	2099	6.73 (d, 15.2), 6.48 (d, 15.2), 6.42 (d, 10.8), 6.31 (d, 11.2), (60:40)	11.6 (2370)	962.2823 (962.0932)	$[M]^{+}$
trans-[$(Et_3P)_2Pt\{C{\equiv}C{-}C_6H_4{-}C_6H_4{-}CH{=}CH(SC_6H_4OMe\text{-}p)\}_2$] (**2b**)	2097	6.92–6.83 (d, merge with SAr-H), 6.53 (d, 13.6), 6.50 (d, 8.8), 6.40 (d, 10.4), (63:37)	11.6 (2396)	1114.3478 (1114.2851)	$[M]^{+}$
trans-[$(Et_3P)_2Pt\{C{\equiv}C{-}C_6H_2(2,5\text{-}Me)_2\text{-}CH{=}CH(SC_6H_4OMe\text{-}p)\}_2$] (**2c**)	2091	6.76 (d, 15.6), 6.66 (d, 15.2), 6.54 (d, 10.4), 6.35 (d, 10.8), (50:50)	12.2 (2384)	1018.3453 (1018.1995)	$[M]^{+}$
trans-[$(Et_3P)_2Pt\{C{\equiv}C{-}C_6H_2(2,5\text{-}OMe)_2\text{-}CH{=}CH(SC_6H_4OMe\text{-}p)\}_2$] (**2d**)	2094	6.90–6.73 (d, d, d, merge with SAr-H), 6.34 (d, 10.4), (65:35)	11.8 (2395)	1082.333258 (1082.1971)	$[M]^{+}$

[a]Referenced to internal TMS

[b] Referenced to external trimethylphosphite and J_{Pt-P} value (in Hz) is given in parentheses

[c]J_{H-H} value (in Hz) is given in parenthesis

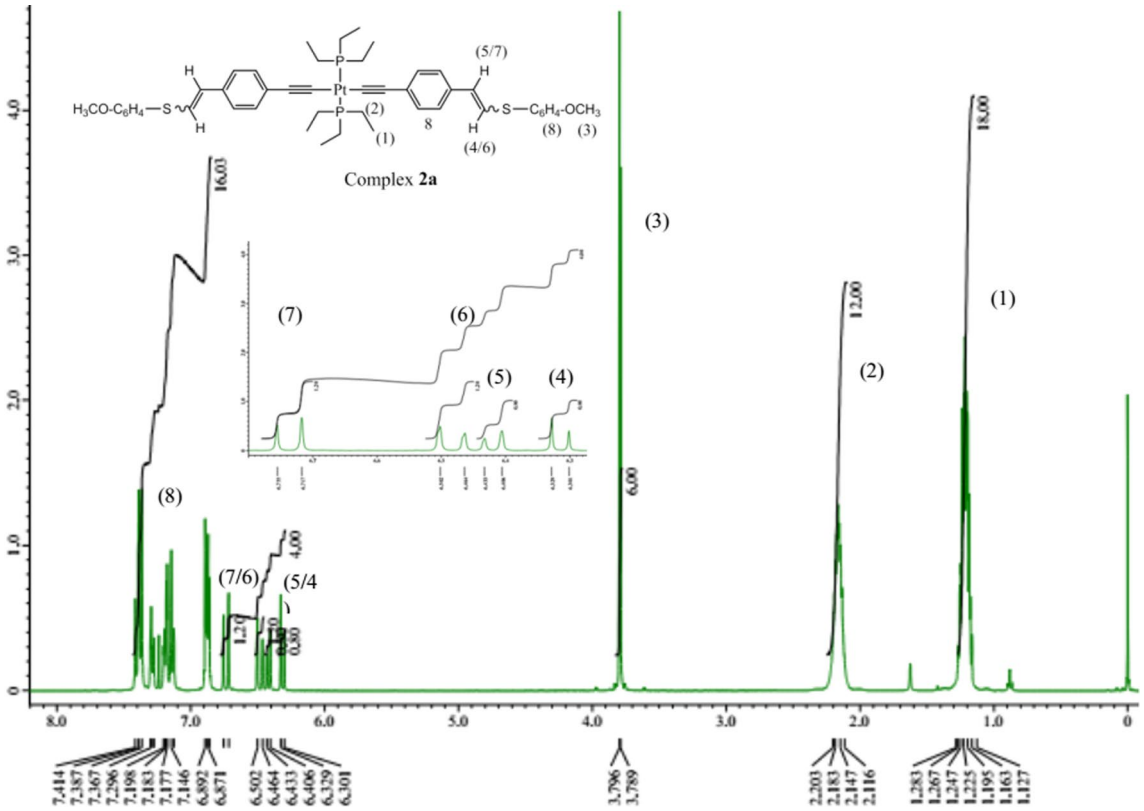

Fig. 1 ^{1}H NMR spectra of Platinum(II) bis(alkenylarylalkynyl) complex **2a**

observed at *m*/*z* 962.2823 for **2a**, at *m*/*z* 1114.3478 for **2b**, at *m*/*z* 1018.3453 for **2c**, and at *m*/*z* 1082.3258 for **2d** (Table 2).

Photophysical properties

The absorption and emission properties of complexes **2a**-**2d** were recorded in THF at room temperature and presented in Fig. 3a, b, c. The platinum(II) bis(alkenylarylalkynyl) complexes of **2a**, **2b**, and **2c** showed the absorption maxima at around ~ 362 nm, whereas **2d** displayed a red-shifted absorption peak at 491 nm due to the presence of an OMe substituent, which releases electrons. All complexes showed a relatively weak peak at around 300 nm. Compared to the absorption band of platinum(II) bis(alkynylarylalkynyl) complexes **1**, we find that the position of the lowest energy absorption bands in the platinum(II) bis(alkenylarylalkynyl) complexes **2** are red-shifted, after the functionalization of *p*-anisolylthiol. The highest red-shift (20 nm) observed for our *trans*-platinum(II) complexes is recorded for complex **2c**. The UV/Vis absorption maxima of complexes **1a**, **1b**, **1c**, and **1d** are observed at 345, 356, 335, and 377 nm, respectively, whereas those of their corresponding *p*-anisolylthiol functionalized complexes **2a**, **2b**, **2c**, and **2d** are observed at 362, 363, 355, and 391 nm, respectively. In each case, a small red-shift is observed, and the shifts are 17, 7, 20, and 14 nm for complexes **2a**, **2b**, **2c**, and **2d**, respectively as compared to complexes **1a**, **1b**, **1c**, and **1d**, respectively. These absorption bands are predominantly based on intraligand charge transfer consisting of acetylenic (C≡C) π–π*, and aromatic and aliphatic (C=C) π–π*transitions [46–49]. The assignment of UV/Vis absorption peaks is further supported by DFT optimized frontier molecular orbitals-HOMO and LUMO of **2a, 2b, 2c** and **2d**. The HOMO is delocalized along the acetylenic, phenyl and ethene π–π*orbitals with a small contribution from the platinum dπ orbital (Fig. 5). The delocalization of the HOMO and LUMO (ground and excited states) is the origin of the red shift of the absorption band of **2d** compared to **2a, 2b** and **2c**. In addition, the excitation energies, along with their related transitions confirmed the presence of HOMO and LUMO in acetylene ligands.

All of the complexes exhibited violet to blue fluorescence emission at room temperature. As complexes **2a**, **2b**, and **2c** showed emission around 405 nm, while **2d** appeared in the blue region (Fig. 3a, b, c). The complexes retained the same fluorescence emission in degassed THF solution, indicating no sign of phosphorescence at room temperature. Low temperature emission spectra were recorded in 2-Me THF to investigate the existence of any triplet state emission in the glassy state. Interestingly, **2a** and **2b** showed intense

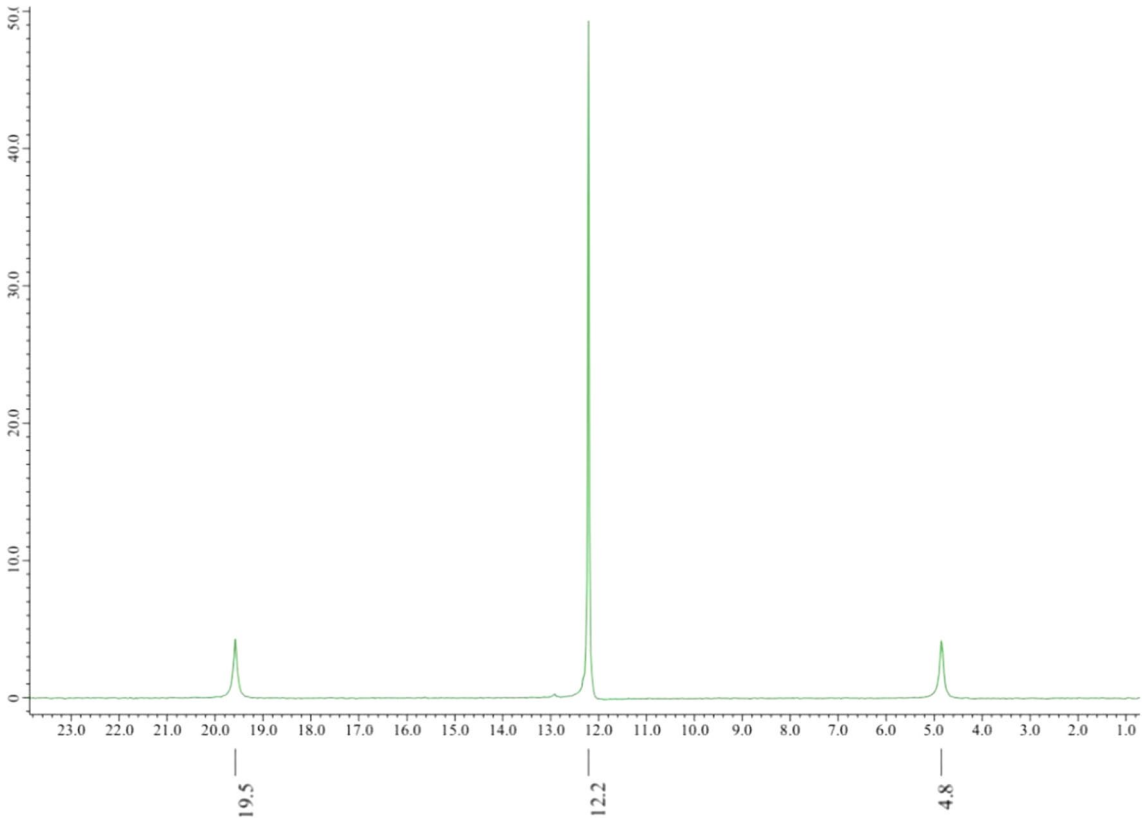

Fig. 2 The $^{31}P\{^{1}H\}$ NMR spectra of platinum(II) bis(alkenylarylalkynyl) complexes **2c**

triplet state emission (phosphorescence) at 579, and 585 nm, respectively with a sharp peak due to the corresponding vibrational relaxation (Fig. 3a, b, c).

However, triplet emission did not show for complexes **2c** and **2d**. It is believed that the substitution of organic spacer with methyl and methoxy groups leading to rises the non-emissive decay from triplet state to ground state at low temperature (77 K), and thereby radiative decay of triplet state to ground state may not observe [50]. Yam VWW et al. (2011) reported that a series of multifunctional platinum(II) bipyridine complexes in which some of examples were alkoxy substituted bipyridine platinum(II) acetylides, that did not show triplet state emission at 77 K [50, 51], but those complexes showed fluorescence at room temperature. In going from room temperature to 77 K, non-radiative decay rate from the triplet state becomes suppressed by the restricted rotational and vibrational motion of the molecules in glassy state [52–55], hence the appearance of phosphorescence for the complexes **2a** and **2b**. The fluorescence lifetime of all four complexes were measured in THF at room temperature. The singlet state fluorescence lifetime for complexes **2a** and **2c** were found at 327 and 322 ps whereas a comparatively shorter lifetime of 309 ps was obtained for complex **2b** (Fig. 3d). However, the excited singlet state lifetime for the complex **2d** was shortened by around half (169 ps), which limits the intersystem crossing between singlet to triplet state significantly. Fluorescence quantum yields (Φ_{fl}) for the complex **2b** and **2d** was higher (~5%) than that of **2a** and **2c** (~2%). The photophysical data is summarized in Table 3.

Electrochemistry

Cyclic voltammetry (CV) is widely used to obtain the highest occupied molecular orbitals (HOMO) and lowest unoccupied molecular orbital (LUMO) energy levels of redox active molecules/polymers [56]. The electrochemical measurements of the complexes **2a**-**2d** were conducted in dichloromethane, in a three electrode system—glassy carbon as working electrode, platinum as auxiliary electrode, and Ag/Ag^{+} in acetonitrile as reference electrode [57]. In all measurements Fc/Fc^{+} (0.18 V vs. Ag/Ag^{+}) were used as internal standard. The CV traces were presented in Fig. 4 and the oxidation potentials were summarized in Table 4. All the complexes exhibited one or more irreversible oxidation waves. The first oxidation waves of **2a**, **2b**, **2c**, and **2d** were observed at 0.47, 0.55, 0.45, and 0.25 V, respectively (Fig. 4 and Table 4). The TD DFT calculations (next section) revealed that the oxidations in the complexes were originated from the acetylide ligands of the complexes (Fig. 5). These oxidations are related to the

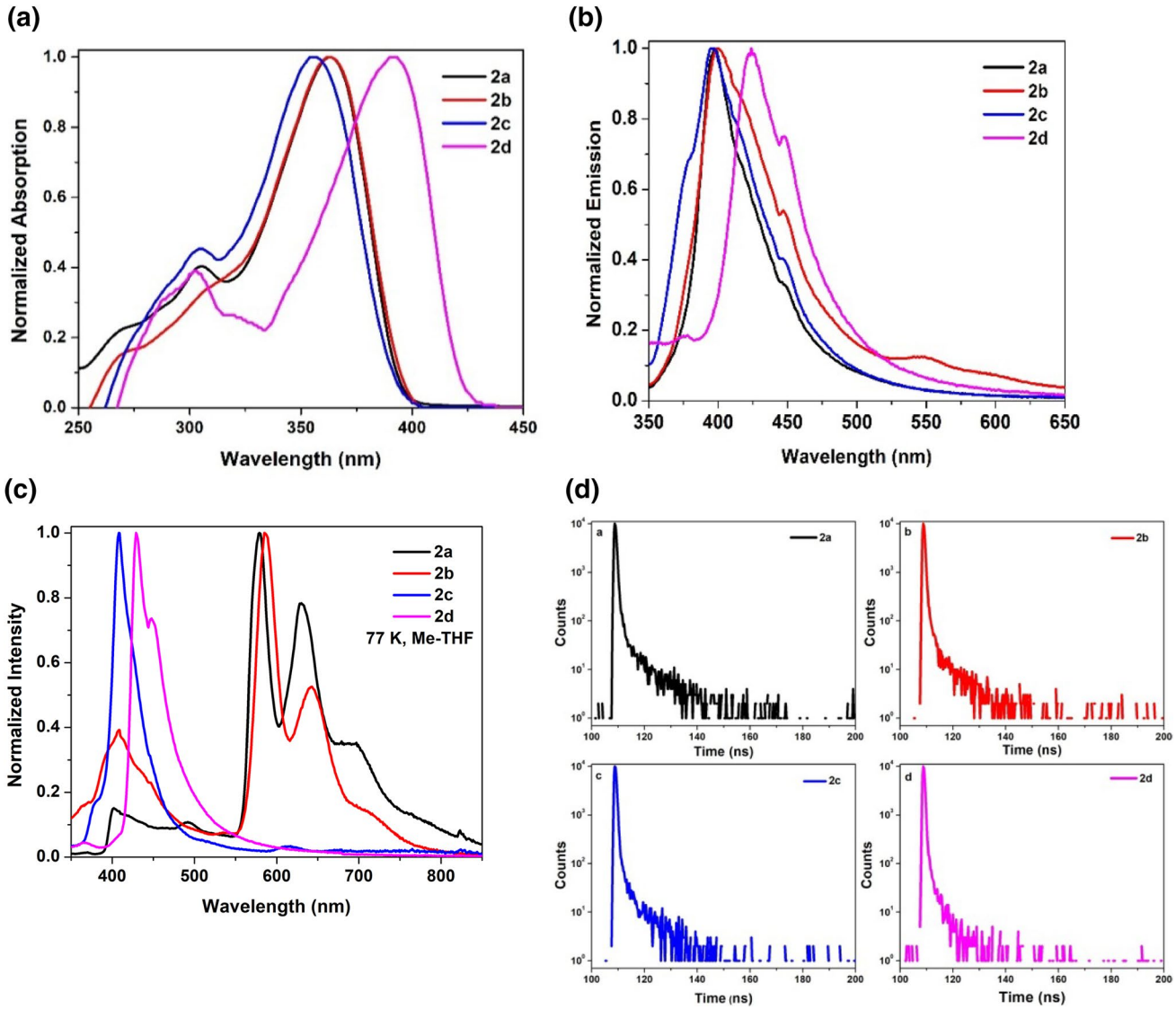

Fig. 3 **a** Absorption spectra in THF **b** room temperature emission spectra in THF **c** emission spectra at 77 K in Me-THF of complexes **2a**-**2d**. **d** fluorescence lifetime decay of complexes **2a**-**2d**

Table 3 Detailed photophysical data of complexes **2a**-**2d**

Compound	Room Temperature			77 K	τ_{Fl} (ps)
	$\lambda_{max\ (nm)}$	Φ_{fl}	$\lambda_{fl\ (nm)}$	$\lambda_{ph\ (nm)}$	
2a	362	2.0%	400	579	327
2b	363	5.5%	407	585	309
2c	355	2.1%	408	–	322
2d	391	4.6%	428	–	169

Conc. = 1.0×10^{-5} M

HOMO energies of the complexes [30, 56, 58]. No reduction was observed within the potential windows (− 2 V to + 2 V). However, LUMO energies of the complexes were obtained from the difference between the HOMO energies and optical gap (E_{opt}). The HOMO and LUMO energies are listed in Table 4.

Theoretical calculations

In order to investigate the electronic structures and energies of frontier molecular orbitals of the complexes (**2a**-**d**), we employed density functional theory (DFT) and time-dependent DFT (TD-DFT) calculations. These calculations utilized the Gaussian 16 program [59] and were based on the hybrid exchange correlation functional B3LYP [60] in conjunction with the Stuttgart–Dresden (SDD) basis set [61]. GaussView, the graphical user interface used with Gaussian software, was employed to visualize the frontier molecular orbitals using an isovalue of 0.02.

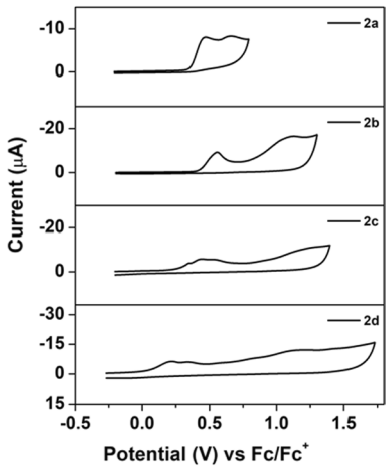

Fig. 4 Cyclic voltammograms of *trans*-[$(PEt_3)_2Pt\{C{\equiv}C–Ar–CH{=}CH(SC_6H_4–OCH_3)\}_2$] (Ar = C_6H_4 (**2a**), Ar = $C_6H_4–C_6H_4$ (**2b**), Ar = C_6H_2(2,5-Me)$_2$, (**2c**) and Ar = C_6H_2(2,5-OMe)$_2$ (**2d**) in dichloromethane using Bu_4NPF_6(0.01 M) as supporting electrolyte

To simplify the computations and reduce the computational cost, the -Et groups on the phosphine ligands were substituted with -Me groups. Figure 5 displays the frontier molecular orbital diagrams for the geometry-optimized complexes (**2a-d**). A visual examination of the orbital plots reveals that the HOMO consists of p orbitals originating from each of the phenylacetylene units and a d orbital localized on the platinum atom. The LUMO consists of p orbitals on the phenylacetylene units and an empty d orbital on the platinum. Analyzing the LUMO images for complexes **2a** and **2c** from Table 5, it is evident that the electron density on one of the phenylacetylene units is notably less than the other, with reduced participation from the d orbital on the platinum atom. The TD-DFT results provided further insight into the basis of the complexes near-UV absorption bands, as demonstrated in Tables 1, 2, 3, and 4 in the SI section. These results indicate that the lowest energy transition exclusively involves the HOMO → LUMO transition. The lowest energy absorption, observed at 362 nm with a significant oscillation strength, precisely corresponds to the experimentally recorded maximum absorption at 362 nm for complex **2a**. For complex **2c**, the theoretically determined lowest energy absorption aligns closely with the experimental result of 355 nm. However, in the case of complexes **2b** and **2d**, the experimental absorptions are lower than the calculated values. Considering the distributions of the frontier orbitals, it is reasonable to conclude that the transition is predominantly $\pi–\pi^*$ in nature with a small degree of metal-to-ligand charge transfer [62].

Conclusions

We have synthesized a series of *p*-anisolylthiol functionalized *trans*-platinum(II) bis(alkenylarylalkynyl) complexes in excellent yield (88–99%) by photochemical reaction. The optical absorption and emission spectra of the complexes are influenced by the nature of spacers in the acetylide ligand. All complexes showed emission bands in the violet-blue region of the electromagnetic spectrum at room temperature. Complexes without any substituents in the phenyl spacer displayed intense triplet state emission (phosphorescence) at low temperature, whereas complexes with substituted phenyl spacers (with CH_3 and OCH_3) did not. The TD-DFT calculations of the complexes shows that the absorption bands are originated from intra-ligand charge transfer ($\pi–\pi^*$) with the participation of platinum dπ-orbital. Cyclic voltammetry (CV) and the TD DFT calculations revealed that the oxidations in the complexes were originated from the acetylide ligands of the complexes. These oxidations are related to the HOMO energies of the complexes.

Table 4 Redox potentials and HOMO and LUMO energies

Complex	$E_{1/2}$[ab]ox /V	$E_{1/2}$ red /V	HOMO/eV	LUMO[c]/eV	ΔE_{opt}[d]/eV	HOMO[e]/eV	LUMO[e]/eV	ΔE_{DFT}/eV
2a	0.47, 0.65	–	−5.27	−2.03	3.24	−4.94	−1.21	3.73
2b	0.55, 0.11	–	−5.35	−2.11	3.24	−5.08	−1.48	3.60
2c	0.45	–	−5.25	−1.95	3.30	−4.86	−1.16	3.70
2d	0.22, 0.11	–	−5.02	−2.0	3.02	−4.57	−1.29	3.28

[a]All potentials are referenced to Fc/Fc^+. HOMO = −(4.8 + E_{ox}); LUMO = −(4.8 + E_{red})

[b]First oxidation

[c]LUMO = HOMO + E_{opt}

[d]$E_{opt.}$is obtained from the intersection of normalized absorption and emission spectra

[e]Obtained from density functional theory calculations

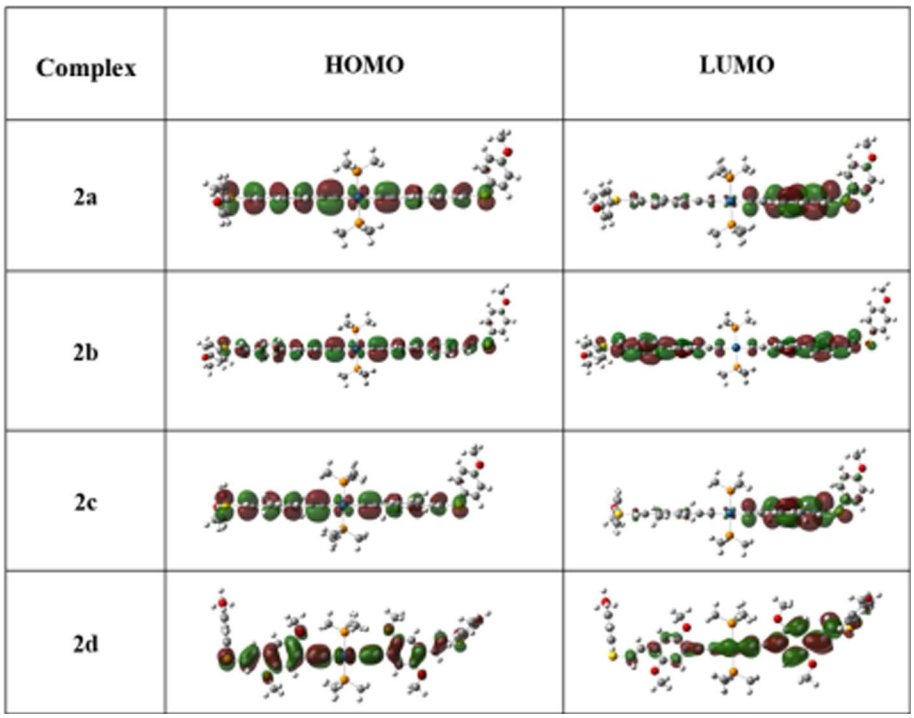

Fig. 5 DFT optimized HOMO-LUMO of **2a**, **2b**, **2c**, and **2d**

Supplementary Information The online version contains supplementary material available at https://doi.org/10.1007/s11243-023-00550-x.

Acknowledgements Rahman MM, Islam T, and Khan MAAT, contributed equally to this work. Corresponding author (Rahman MM) e-mail: mostafiz-che@sust.edu. We would like to thank the Research Center of Shahjalal University of Science & Technology for its generous support for funding (PS/2018/2/15). We also acknowledge the funding from Higher Education Quality Enhancement Project (HEQEP) of the University Grants Commission of Bangladesh for purchasing the FT-IR and UV–vis spectrometer. We are grateful to Dr. Kirk Schanze of the University of Texas at San Antonio, San Antonio, Texas, USA for his generous support, providing us with instrumental facilities for low temperature PL measurement and excited state lifetime measurements.

Author contributions MR: Methodology, writing—review & editing, Writing—original draft, Conceptualization. TI: Methodology & writing (DFT & CV). AATK: Methodology & writing (Photophysical). MY: Review & editing. DP: Review & editing. SJ: Methodology. AO: Review & editing.

Declarations

Competing interests The authors declare no competing interests.

References

1. Haque A, Al-Balushi RA, Al-Busaidi IJ, Khan MS, Raithby PR (2018) Chem Rev 118:8474–8597
2. Wong WY, Ho CL (2006) Coord Chem Rev 250:2627–2690
3. Zhou GJ, Wong WY (2011) Chem Soc Rev 40:2541–2566
4. Xu LJ, Zeng XC, Wang JY, Zhang LY, Chi Y, Chen ZN (2016) ACS Appl Mater Interfaces 8:20251–20257
5. Bullock JD, Xu Z, Valandro S, Younus M, Xue J, Schanze KS (2020) ACS Appl Electron Mater 2:1026–1034
6. Li Y, Tong H, Xie Z, Wang L (2013) Polym Chem 4:2884–2890
7. Holt ED, Wang J, Winkel RW, Younus M, Schanze KS (2021) Photo Chem Photo Bio 8:100060. https://doi.org/10.1016/j.jpap.2021.100060
8. Wong WY, Ho CL (2010) Acc Chem Res 43:1246–1256
9. Yan L, Zhao Y, Wang X, Wang XZ, Wong WY, Liu Y, Wu W, Xiao Q, Wang G, Zhou X, Zeng W, Li C, Wang X, Wu H (2012) Macromol Rapid Commun 33:603–609
10. Durand RJ, Gauthier S, Achelle S, Kahlal S, Saillard JY, Barsella A, Wojcik L, Poul NL, Guen FRL (2017) Dalton Trans 46:3059–3069
11. Goswami S, Cekli S, Alarousu E, Winkel RW, Younus M, Mohammed OF, Schanze KS (2020) Macromolecules 53:6279–6287
12. Tam AYY, Wong KMC, Yam VWW (2009) J Am Chem Soc 131:6253–6260
13. Camerel F, Ziessel R, Donnio B, Bourgogne C, Guillon D, Schmutz M, Lacovita C, Bucher JP (2007) Angew Chem Int Ed 46:2659–2662
14. Takahashi S, Murata E, Kariya M, Sonogashira K, Hagihara N (1979) Macromolecules 12:1016–1018
15. Spencer M, Santoro A, Freeman GR, Díez Á, Murray PR, Torroba J, Whitwood AC, Yellowlees LJ, Williams JAG, Bruce DW (2012) Dalton Trans 41:14244–14256
16. Younus M, Köhler A, Cron S, Chawdhury N, Al-Mandhary MRA, Khan MS, Long NJ, Friend RH, Raithby PR (1998) Angew Chem Int Ed 37:3036–3039
17. Goswami S, Hernandez JL, Gish MK, Wang J, Kim B, Laudari AP, Guha S, Papanikolas JM, Reynolds JR, Schanze KS (2017) Chem Mater 29:8449–8461
18. Hilderbrandt A, Kovalski E, Korb M (2021) Eur J Inorg Chem 2021(25):2523–2532

19. Beljonne D, Wittmann HF, Köhler A, Graham S, Younus M, Lewis J, Raithby PR, Khan MS, Friend RH, Brédas JL (1996) J Chem Phys 105:3868–3877
20. Silverman EE, Cardolaccia T, Zhao X, Kim KY, Haskins-Glusac K, Schanze KS (2005) Coord Chem Rev 249:1491–1500
21. Hagihara N, Sonogashira K, Takahashi S (1981) Adv Poly Sci 41:149–179
22. Liu L, Zhang C, Zhao J (2014) Dalton Trans 43:13434–13444
23. Lara R, Lalinde E, Moreno M (2017) Dalton Trans 46:4626–4641
24. Mullin WJ, Qin H, Mani T, Muller P, Panzer MJ, Thomas SW (2020) Chem Commun 56:6854–6857
25. Sonogashira K, Fujikura Y, Yatake T, Toyoshima N, Takahashi S, Hagihara N (1978) J Organomet Chem 145:101–108
26. Khan MS, Davies SJ, Kakkar AK, Schwartz D, Lin B, Johnson BFG, Lewis J (1992) J Organomet Chem 424:87–97
27. Scattergood PA, Delor M, Sazanovich IV, Bouganov OV, Tikhomirov SA, Stasheuski AS, Parker AW, Greetham GM, Towrie M, Davies ES, Meijer AJHM, Weinstein JA (2014) Dalton Trans 43:17677–17693
28. Wong HL, Tao CH, Zhu N, Yam VWW (2011) Inorg Chem 50:471–481
29. Nishijo J, Uchida M, Enomoto M, Akita M (2021) Transit Met Chem 46:373–380
30. Younus M, Valandro S, Gobeze HB, Ahmed S, Schanze KS (2023) J Photochem Photobiol, A 435:114303
31. Rahman MM, Nomoto A, Younus M, Ogawa A (2014) Eur J Inorg Chem 2014(16):2613–2617
32. Rahman MM, Younus M, Ogawa A (2015) Eur J Inorg Chem 2015(8):1340–1344
33. Ichinose Y, Wakamatsu K, Nozaki K, Birbaum JL, Oshima K, Utimoto K (1987) Chem Lett 16(8):1647–1650
34. Wille U (2013) Chem Rev 113:813–853
35. Rahman MM, Younus M, Ogawa A (2014) RSC Adv 4:25389–25392
36. Rahman MM, Younus M, Naher M, Masud MK, Nomoto A, Ogawa A, Rudnick A, Köhler A (2016) J Organomet Chem 818:185–194
37. Rahman MM, Pramanik SK, Paul D, Sarkar M, Ahmed MJ, Saha R, Ogawa A (2019) Transit Metal Chem 44:247–252
38. Cardolaccia T, Li Y, Schanze KS (2008) J Am Chem Soc 130:2535–2545
39. Dai FR, Chen YC, Lai LF, Wu WJ, Cui CH, Tam GP, Wang XZ, Lin JT, Tian H, Wong WY (2012) Chem Asian J 7:1426–1434
40. Armarego WLF, Perrin DD (1996) Purification of Laboratory Chemicals, 4th edn. Butterworth-Heinemann, Guildford
41. Takahashi S, Kuroyama Y, Sonogashira K, Hagihara N (1980) Synthesis 1980(8):627–630
42. Oliver TAA, King GA, Tew DP, Richard ND, Ashfold MNR (2012) J Phys Chem A 116:12444
43. Riduan SN, Ying JY, Zhang Y (2012) Org Lett 14:1780–1783
44. Grim SO, Keiter RL, McFarlane W (1967) Inorg Chem 6:1133–1137
45. Rieger AL, Carpenter GB, Rieger PH (1993) Organometallics 12:842–847
46. Khan MS, Al-Mandhary MRA, Al-Suti MK, Feeder N, Nahar S, Kohler A, Friend RH, Wilson PJ, Raithby PR (2002) J Chem Soc Dalton Trans 12:2441–2448
47. Liu Y, Jiang S, Glusac K, Powell DH, Anderson DF, Schanze KS (2002) J Am Chem Soc 124:12412–12413
48. D'Amato R, Furlani A, Colapietro M, Portalone G, Casalboni M, Falconieri M, Russo MV (2001) J Organomet Chem 627:13–22
49. Ahmad MF, Rahman MM, Khan MAAT, Siddique AB, Ara MH, Biswas MK, Bhoumik NC, Ghosh S, Jagadesan P, Khan MMR, Younus M (2021) J Organomet Chem 950:121970
50. Li Y, Tam AYY, Wong KMC, Li W, Wu L, Yam VWW (2011) Chem Eur J 17:8048–8059
51. Ko CC, Wu L, Wong KMC, Zhu N, Yam VWW (2004) Chem Eur J 10:766–776
52. Baroncini M, Bergamini G, Ceroni P (2017) Chem Commun 53:2081–2093
53. Reineke S, Baldo MA (2014) Sci Rep 4:3797
54. Amin MK, Rahman MM, Naher M, Islam T, Ahmad MF, Khan MA, Khan MMR, Alam MA, Younus M, Biswas MK, Haque Y (2017) Synth Met 232:96–102
55. Ahmed MK, Rahman MM, Naher M, Mehdi SS, Khan AR, Khan MMR, Islam SMS, Younus M, Wedler S, Bagnich S, Hofmann AL, Rudnick A, Köhler A (2019) Macromol Chem Phys 220:1800494
56. Cardona CM, Li W, Kaifer AE, Stockdale D, Bazan GC (2011) Adv Mater 23:2367–2371
57. Elgrishi N, Rountree KJ, McCarthy BD, Rountree ES, Eisenhart TT, Dempsey JL (2018) J Chem Educ 95:197–206
58. Dai F-R, Zhan H-M, Liu Q, Fu Y-Y, Li J-H, Wang Q-W, Xie Z, Wang L, Yan F, Wong W-Y (2012) Chem Eur J 18:1502–1511
59. Frisch MJ, Trucks GW, Schlegel HB, Scuseria GE, Robb MA, Cheeseman JR, Scalmani G, Barone V, Petersson GA, Nakatsuji H, Li X, Caricato M, Marenich AV, Bloino J, Janesko BG, Gomperts R, Mennucci B, Hratchian HP, Ortiz JV, Izmaylov AF, Sonnenberg JL, Williams-Young D, Ding F, Lipparini F, Egidi F, Goings J, Peng B, Petrone A, Henderson T, Ranasinghe D, Zakrzewski VG, Gao J, Rega N, Zheng G, Liang W, Hada M, Ehara M, Toyota K, Fukuda R, Hasegawa J, Ishida M, Nakajima T, Honda Y, Kitao O, Nakai H, Vreven T, Throssell K, Montgomery JA Jr, Peralta JE, Ogliaro F, Bearpark MJ, Heyd JJ, Brothers EN, Kudin KN, Staroverov VN, Keith TA, Kobayashi R, Normand J, Raghavachari K, Rendell AP, Burant JC, Iyengar SS, Tomasi J, Cossi M, Millam JM, Klene M, Adamo C, Cammi R, Ochterski JW, Martin RL, Morokuma K, Farkas O, Foresman JB, Fox DJ (2016) Gaussian 16, Revision C.01. Gaussian Inc, Wallingford
60. Becke AD (1993) J Chem Phys 98:5648–5652
61. Andrae D, Häußermann U, Dolg M, Stoll H, Preuß H (1990) Theoret Chim Acta 77:123–141
62. Cooper TM, Krein DM, Burke AR, McLean DG, Rogers JE, Slagle JE (2006) J Phys Chem A 110:13370–13378